LCAT can Rescue the Abnormal Phenotype Produced by the Natural ApoA-I Mutations $(Leu141Arg)_{Pisa}$ and $(Leu159Arg)_{FIN}$[†]

Georgios Koukos,[‡,§,||] Angeliki Chroni,[⊥] Adelina Duka,[‡] Dimitris Kardassis,[§,#] and Vassilis I. Zannis*[,‡,§]

Molecular Genetics, Departments of Medicine and Biochemistry, Whitaker Cardiovascular Institute, Boston University School of Medicine, Boston, Massachusetts 02118, Department of Basic Sciences, University of Crete Medical School, Heraklion, GR-71110, Greece, Institute of Biology, National Center for Scientific Research "Demokritos", 15310 Agia Paraskevi, Athens, Greece, and Institute of Molecular Biology and Biotechnology, FORTH, Heraklion, Crete, Greece

Received February 14, 2007; Revised Manuscript Received May 22, 2007

ABSTRACT: To explain the etiology and find a mode of therapy of genetically determined low levels of high-density lipoprotein (HDL), we have generated recombinant adenoviruses expressing apolipoprotein A-I (apoA-I)$(Leu141Arg)_{Pisa}$ and apoA-I$(Leu159Arg)_{FIN}$ and studied their properties *in vitro* and *in vivo*. Both mutants were secreted efficiently from cells but had diminished capacity to activate lecithin/cholesterol acyltransferase (LCAT) *in vitro*. Adenovirus-mediated gene transfer of either of the two mutants in apoA-I-deficient (apoA-$I^{-/-}$) mice resulted in greatly decreased total plasma cholesterol, apoA-I, and HDL cholesterol levels. The treatment also decreased the cholesteryl ester to total cholesterol ratio (CE/TC), caused accumulation of preβ1-HDL and small size α4-HDL particles, and generated only few spherical HDL particles, as compared to mice expressing wild-type (WT) apoA-I. Simultaneous treatment of the mice with adenoviruses expressing either of the two mutants and human LCAT normalized the plasma apoA-I, HDL cholesterol levels, and the CE/TC ratio, restored normal preβ- and α-HDL subpopulations, and generated spherical HDL. The study establishes that apoA-I$(Leu141Arg)_{Pisa}$ and apoA-I$(Leu159Arg)_{FIN}$ inhibit an early step in the biogenesis of HDL due to inefficient esterification of the cholesterol of the preβ1-HDL particles by the endogenous LCAT. Both defects can be corrected by treatment with LCAT.

ApoA-I[1] is the main protein component and is required for the biogenesis and functions of HDL (*2*−*4*). HDL is synthesized through a complex pathway that involves various membrane-bound proteins, plasma enzymes, and lipid-transfer proteins (*5*). HDL assembles by an initial ABCA1-mediated transfer of cellular phospholipids and cholesterol to extracellular lipid-poor apoA-I acceptor. The initial lipidation of apoA-I is followed by remodeling in the plasma compartment of HDL particles by esterification of cholesterol by the enzyme LCAT, the exchange between HDL and other lipoproteins of apolipoproteins and lipids as well as the putative transfer of additional cellular cholesterol to the growing particles by the scavenger receptor class B type I (SR-BI) (*6*) and the cell surface transporter ABCG1 (*7*). Hydrolysis of lipids of HDL is mediated by various lipases (lipoprotein lipase, hepatic lipase, and endothelial lipase) (*5*) and exchange of lipids by the phospholipid transfer protein (PLTP) (*8*) and by the cholesteryl ester transfer protein (CETP) (*9*).

Several naturally occurring apoA-I mutations that produce pathological phenotypes have been described (*5*, *10*−*14*). In recent studies, we have shown that mutations in apoA-I may affect different steps in the biogenesis of HDL or cause dyslipidemia (*15*−*19*). It has been estimated that structural mutations of apoA-I occur in 0.3% of the Japanese population and may affect the plasma HDL levels (*20*). From a total of 46 natural mutations of apoA-I, 25 are associated with low HDL levels, and 17 of these mutants reduce the capacity of apoA-I to activate LCAT (*5*, *12*). These mutations are clustered predominantly in or at the vicinity of helix 4 of apoA-I (*21*) and some of them predispose to atherosclerosis (*10*, *11*, *13*, *14*, *22*).

In the current study, we investigated the effect of two naturally occurring apoA-I mutations, apoA-I$(Leu141Arg)_{Pisa}$ and apoA-I$(Leu159Arg)_{FIN}$, on the biogenesis of HDL. These mutations have been associated with very low HDL cholesterol and apoA-I levels as well as hypo-α lipoproteinemia

[†] This work was supported by the National Institutes of Health Grant (HL48739), the 6th Framework Programme of the European Union (No. LSHM-CT-2006-037631), and a grant from the Ministry of Education and the Ministry of Development of Greece (PENED 2001).

* To whom correspondence should be addressed. Tel: 617-638-5085. Fax: 617-638-5141. E-mail: vzannis@bu.edu.

[‡] Boston University School of Medicine.

[§] University of Crete Medical School.

[||] Graduate student of the Joint Graduate Program in Molecular Biology and Biomedicine of the Department of Biology and the Basic Science Department of the University of Crete Medical School.

[⊥] National Center for Scientific Research "Demokritos".

[#] FORTH.

[1] Abbreviations: ABCA1, ATP binding cassette transporter A1; apoA-I, apolipoprotein A-I; apoA-$I^{-/-}$ mice, apoA-I-deficient mice; BSA, bovine serum albumin; CE, cholesteryl ester; CETP, cholesteryl ester transfer protein; cpt-cAMP, 8-(4-chlorophenylthio) adenosine 3′:5′-cyclic monophosphate; EM, electron microscopy; FBS, fetal bovine serum; GFP, green fluorescent protein; HDL, high density lipoprotein; LCAT, lecithin/cholesterol acyltransferase; SDS−PAGE, sodium dodecyl sulfate−polyacrylamide gel electrophoresis; PBS, phosphate-buffered saline; pfu, plaque forming units; PLTP, phospholipid transfer protein; SR-BI, scavenger receptor class B type I; TC, total cholesterol; WT, wild-type.

10.1021/bi7003203 CCC: $37.00
Published on Web 08/21/2007

Table 1: Oligonucleotide Sequence of Primers Used in PCR Amplifications

primer name[a]	primer sequence	nucleotide mutation[b]
apoAIg F	5′ - GCTCTAGATCTGACATAAATAGGCCCTGC - 3′	
apoAIg R	5′ - GCGGATATCCAGGCCTTGTTTGAGCC - 3′	
L141R apoAI F	5′ - CTGCAAGAGAAG **CGG**[c] AGCCCACTGGGC - 3′	T-1009-G
L141R apoAI R	5′ - GCCCAGTGGGCT CCG CTTCTCTTGCAG - 3′	
L159R apoAI F	5′ - CATGTGGACGCG **CGG** CGCACGCATCTG - 3′	T-1063-G
L159R apoAI R	5′ - CAGATGCGTGCG CCG CGCGTCCACATG - 3′	

[a] Amino acid position refers to the mature plasma apoA-I protein sequence. [b] Nucleotide number of the human apoA-I genomic sequence (*1*) relative to the translation initiation ATG codon. [c] Codon encoding the mutation is shown in bold.

in human subjects (*13*, *22*−*27*). Using adenovirus-mediated gene transfer of these mutants in apoA-I$^{-/-}$ mice, we found that both mutations fail to form discoidal or spherical HDL particles and are associated with very low plasma HDL levels. These defects could be corrected by co-infection of mice with adenoviruses expressing the mutant proteins along with human LCAT, indicating that the endogenous LCAT was insufficient to esterify the cholesterol of preβ-HDL and thus to promote the sequential conversion of the preβ-HDL particles to discoidal and spherical HDL particles.

EXPERIMENTAL PROCEDURES

Materials. Materials not mentioned in the Experimental Procedures have been obtained from sources described previously (*15*, *19*).

Generation of Adenoviruses Expressing the Wild-Type (WT) and the Mutant ApoA-I Forms. Initially, the pUC19-apoAIg plasmid (*28*) was digested with BglII and treated with the Klenow fragment of DNA polymerase I to fill the recessed 3′-end and ligated in order to eliminate the BglII site. The derivative plasmid, designated pUC19-apoAIg-(ΔBglII), was used as a template to amplify the human apoA-I genomic sequence by PCR. For the amplification, a set of 5′- and 3′-flanking primers designated apoAIg F and apoAIg R was used (Table 1). The first primer was designed to carry the XbaI (5′-TCTAGA-3′) and BglII (5′-AGATCT-3′) recognition sites, and the second primer carried the EcoRV (5′-GATATC-3′) recognition site incorporating them to the 5′ and 3′ of the apoA-I genomic sequence, respectively. The product of PCR was cloned into the pCDNA3.1 vector, resulting in the generation of the vector pCDNA3.1-apoAIg-(ΔBglII). The apoA-I mutants described in this study were generated using the mutagenesis kit QuikChange XL (Stratagene). The mutagenic primers used are shown in Table 1. In all mutagenesis reactions, the pCDNA3.1-apoA-Ig(ΔBglII) vector containing the genomic sequence of the human apoA-I was used as a template. Following 18 cycles of PCR amplification of the template DNA, the PCR product was treated with DpnI to digest the parental plasmids containing methylated DNA in one or both strands. The reaction product containing newly synthesized DNA carrying the mutations of interest was used to transform competent cells XL10-Gold (Stratagene). Ampicillin-resistant clones were selected, and plasmid DNA was isolated from these clones and subjected to sequencing to verify the presence of the desired point mutation. The plasmid containing the mutation of interest was digested with BglII and EcoRV, and the 2.2 kb insert was subcloned into the BglII and EcoRV sites of the pAdTrackCMV vector to generate recombinant adenoviruses according to the Ad-Easy-1 system (Stratagene). The adenovirus construct was generated in bacteria BJ-5183-pAD1 (Stratagene). Correct clones were propagated in DH5a bacterial cells. The recombinant adenoviral vectors were linearized after incubation with PacI and used to transfect 911 cells. Following a large-scale infection of human embryonic kidney 293 cell cultures, the recombinant adenoviruses were purified by two consecutive $CsCl_2$ ultracentrifugation steps, dialyzed, and titrated.

Cell Secretion of WT and Mutant apoA-I Forms. To assess the secretion of WT and mutant apoA-I forms, HTB13 cells (SW 1783 human astrocytoma) grown to 80% confluence in Leibovitz's L-15 medium containing 2% heat-inactivated horse serum in 100 mm diameter dishes were infected with adenoviruses expressing WT and mutant apoA-I forms at a multiplicity of infection (moi) of 20. Twenty-four hours post-infection, the cells were washed twice with phosphate-buffered saline (PBS) and incubated in serum-free medium for 2 h. Following an additional wash with PBS, fresh serum-free medium was added, and after 24 h of incubation, medium was collected and analyzed by SDS−PAGE for apoA-I expression.

Production and Purification of WT and Mutant apoA-I Forms Using the Adenovirus System. ApoA-I was purified from the culture medium of HTB13 cells grown in roller-bottles. The cells were infected with the adenoviruses expressing apoA-I(Leu141Arg)$_{Pisa}$ or apoA-I(Leu159Arg)$_{FIN}$. The medium was harvested every 24 h after infection, and the protein was purified as described (*29*).

LCAT Activation Assay. LCAT was purified as described (*19*) from the culture medium of human HTB13 cells infected with an adenovirus expressing the human LCAT cDNA (*30*). The reconstituted HDL (rHDL) particles used as the substrate contained cholesterol and [^{14}C]-cholesterol ([4-^{14}C] cholesterol, 0.04 mCi/mL, specific activity of 45 mCi/mmol; Perkin-Elmer Life Sciences, Inc.), β-oleoyl-γ-palmitoyl-L-α-phosphatidylcholine (POPC) and apoA-I and were prepared by the sodium cholate dialysis method as described previously (*31*). rHDL particles without [^{14}C]-choletserol containing mutant forms of apoA-I were prepared with the same procedure in order to measure their size by EM. The size of these particles was determined from the negatives of the EM image as described (*32*). The LCAT activity of the plasma of mice, 4 days after infection with adenoviruses expressing the mutant apoA-I(Leu141Arg)$_{Pisa}$ alone or in combination with the human LCAT, was determined as described above using plasma samples instead of purified LCAT and rHDL particles containing WT apoA-I as substrate. For mice expressing apoA-I(Leu141Arg)$_{Pisa}$, 4 μL of plasma were used, while for mice expressing the combination of the mutant apoA-I and human LCAT, 0.4 μL of plasma were used. The

enzymatic reactions were carried out as described, and the apparent *V*max and *K*m were derived as described previously (*17*).

ABCA1-Dependent Cholesterol Efflux Assay. ABCA1-dependent efflux of [^{14}C]-cholesterol was measured using J774 macrophages, in which the expression of ABCA1 was induced by a cAMP analogue, using WT and mutant apoA-I forms as cholesterol acceptors. The J774 mouse macrophages were grown in DMEM containing 4.5 g/L glucose and 10% (v/v) FBS and antibiotics, labeled with 8 μCi/mL [4-^{14}C]-cholesterol for 24 h, and then treated with 0.3 mM cpt-cAMP for 24 h. Cholesterol efflux was determined as described previously (*15*).

Animal Studies, Plasma Lipids, and ApoA-I. ApoA-I$^{-/-}$ (ApoA-I^{tm1Unc}) C57BL/6J mice (*3*) were purchased from Jackson Laboratories (Bar Harbor, ME). The mice were maintained on a 12 h light/dark cycle and standard rodent chow. All procedures performed on the mice were in accordance with National Institutes of Health and institutional guidelines. ApoA-I$^{-/-}$ mice 6−8 weeks of age were injected via the tail vein with $1-2 \times 10^9$ pfu of recombinant adenovirus per animal, and the animals were sacrificed 4 days post-injection following a 4 h fast. The concentration of total cholesterol, free cholesterol, phospholipids, and triglycerides of plasma drawn 4 days post-infection was determined using the cholesterol E, free cholesterol C, and phospholipids B reagents (Wako Chemicals Inc.), and INFINITY triglycerides reagent (ThermoDMA), respectively, according to the manufacturer's instructions. The concentration of cholesteryl esters was determined by subtracting the concentration of free cholesterol from the concentration of total cholesterol. Plasma apoA-I levels were determined using AutoKit-AI (Wako Chemicals Inc.). For FPLC analysis of plasma, 17 μL of plasma obtained from mice infected with adenovirus-expressing WT or mutant apoA-I forms were loaded onto a Sepharose 6 PC column in a SMART microFPLC system (Amersham Biosciences) and eluted with PBS. A total of 25 fractions of 50 μL volume each were collected for further analysis. The concentration of lipids in the FPLC fractions was determined as described above.

Fractionation of Plasma by Density Gradient Ultracentrifugation and Electron Microscopy (EM) Analysis of the ApoA-I Containing Fractions. For this analysis, 300 μL of plasma obtained from adenovirus-infected mice was fractionated by density gradient ultracentrifugation as described (*17*). Aliquots of 100 μL from each fraction were subjected to SDS−PAGE, and the protein bands were visualized by staining with Coomassie Brilliant Blue. For EM analysis, the fractions that float in the HDL region were treated and photographed as described (*17*).

Nondenaturating Two-Dimensional (2D) Gel Electrophoresis. The distribution of HDL subfractions in plasma was analyzed by 2D electrophoresis as described (*17*). The proteins were transferred to a nitrocellulose membrane, and apoA-I was detected by using the goat polyclonal anti-human apoA-I antibody AB740 (Chemicon International).

RNA Isolation and Hybridization Analysis. Total RNA was isolated from liver tissue of mice 4 days post-infection, using Tirzol (Invitrogen), according to the manufacturer's instructions. RNA was analyzed by Northern blotting, and the apoA-I and GAPDH mRNA bands were detected and quantitated as described (*19*).

RESULTS

Protein Expression and the Ability of Mutant ApoA-I Forms to Activate LCAT and Promote ABCA1-Mediated Cholesterol Efflux in Vitro. We have generated recombinant adenoviruses expressing the WT apoA-I and the apoA-I(Leu141Arg)$_{Pisa}$ and apoA-I(Leu159Arg)$_{FIN}$ mutants that were found in human patients (*13*, *22*, *24*−*27*). To assess the expression and secretion of the two mutants compared to WT apoA-I, we infected HTB13 cells grown in 5 mL of medium in 100 mm diameter dishes with recombinant adenoviruses harboring the WT or the mutant apoA-I genes using an moi of 20. Analysis of the cultured media 24 h post-infection showed that the WT apoA-I, apoA-I(Leu141Arg)$_{Pisa}$, and apoA-I(Leu159Arg)$_{Fin}$ were secreted at a rate of 173, 139, and 159 μg/mL/24 h, respectively, indicating that the secretion of the WT and the two mutants was comparable (Figure 1A). For the LCAT activation, WT and the two mutant forms of apoA-I produced by the adenovirus expression system were purified and used for the generation of rHDL particles as described (*18*, *19*). The size of the rHDL particles was determined from the negatives of the EM images. The particles have a diameter of 13.7 ± 3.9 nm and a thickness of 5.4 nm. The molar ratio of POPC/cholesterol/apoA-I of the discoidal particles is 60:8:1, respectively. LCAT activity was assayed as the rate of production of labeled cholesteryl esters from the ^{14}C-labeled rHDL particles. The esterification of the cholesterol of the rHDL particles containing the apoA-I(Leu141Arg)$_{Pisa}$ and apoA-I(Leu159Arg)$_{FIN}$ mutants was very low and could be overcome by excess LCAT. It was found that a 20-fold increase in enzyme concentration resulted in an initial velocity of esterification comparable to that obtained with normal apoA-I using 1-fold enzyme concentration. Using this enzyme concentration, the *K*m$_{app}$ and *V*max$_{app}$ values of the mutants were calculated and compared to those of the WT apoA-I and are shown in Figure 1B. Compared to WT apoA-I, mutant apoA-I(Leu141Arg)$_{Pisa}$ had greatly reduced *V*max$_{app}$ values and normal *K*m$_{app}$ values, whereas mutant apoA-I(Leu159Arg)$_{FIN}$ had greatly reduced *V*max$_{app}$ and a 3.5-fold increase in *K*m$_{app}$ (Figure 1B). These findings are compatible with previously published data (*13*, *23*, *33*). The ability of apoA-I(Leu141Arg)$_{Pisa}$ and apoA-I(Leu159Arg)$_{FIN}$ to promote ABCA1-mediated cholesterol efflux was determined using J774 mouse macrophages that were stimulated by the cAMP analogue, cpt-cAMP. The net cpt-cAMP-dependent cholesterol efflux from J774 macrophages using the mutant proteins as cholesterol acceptors was obtained by subtracting the efflux values of the untreated cells from the efflux values of the cpt-cAMP-treated cells after 4 h of incubation. The efflux values obtained for WT apoA-I were set to 100%. This analysis showed that the cpt-cAMP-dependent (ABCA1-mediated) cholesterol efflux in the presence of apoA-I(Leu141Arg)$_{Pisa}$ acceptor was 86% and in the presence of apoA-I(Leu159Arg)$_{FIN}$ acceptor was 113% of the WT control (Figure 1C). Previous studies indicated that the capacity of apoA-I(Leu159Arg)$_{FIN}$ to promote cholesterol efflux from J774 macrophages was similar to that of WT apoA-I (*33*).

Plasma Lipid, ApoA-I, and Hepatic ApoA-I mRNA Levels Following Adenovirus Infection. Mice were injected with doses ranging from $1-2 \times 10^9$ pfu in order to achieve hepatic mRNA levels that were comparable to the WT apoA-I

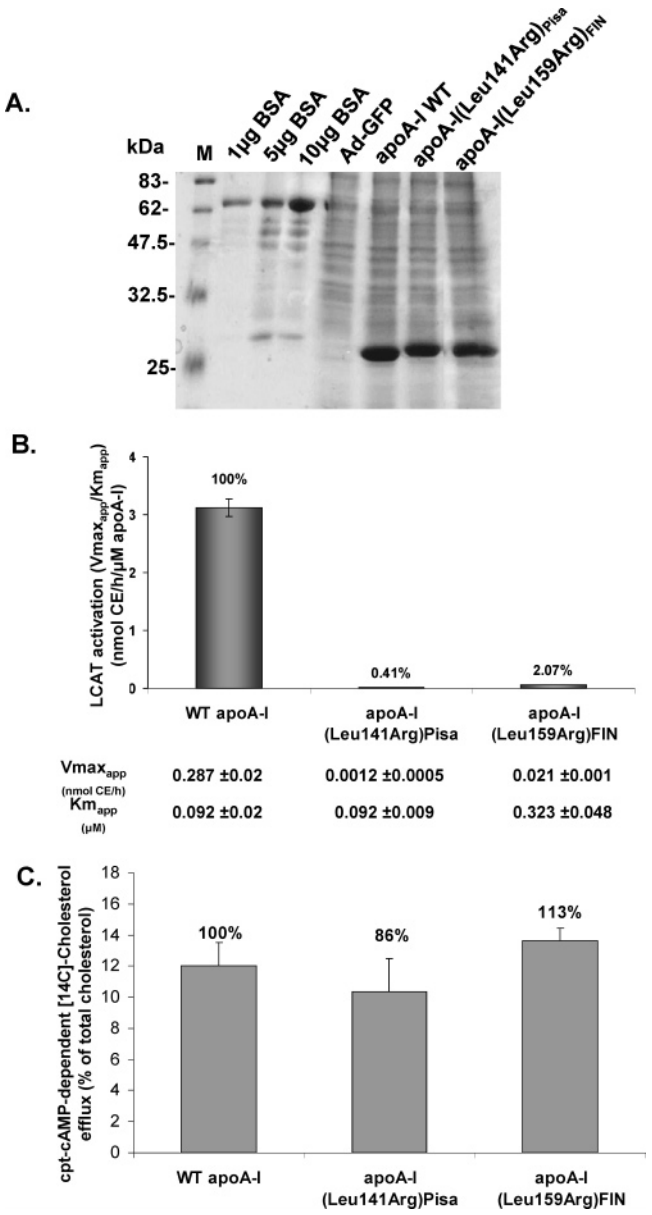

FIGURE 1: (A−C) ApoA-I expression and in vitro functional assays. Panel A: SDS−PAGE analysis of 100 μL of culture medium of HTB13 cells infected with control adenovirus expressing GFP and adenoviruses expressing WT and mutant apoA-I forms. Panel B: Activation of LCAT by rHDL containing WT or mutant apoA-I forms. The apparent *K*m and *V*max values of the reaction are shown on the bottom of the figure. The catalytic efficiency ($Vmax_{app}/Km_{app}$) values on the *y*-axis are the means ± S.D. from three independent experiments performed in duplicate. Panel C: ABCA1-mediated cholesterol efflux in the presence of WT apoA-I and apoA-I(Leu141Arg)$_{Pisa}$, and apoA-I(Leu159Arg)$_{FIN}$ was determined as described in Experimental Procedures.

mRNA expression levels. The different doses of the mutant forms were used to look for potential changes in the observed phenotypes as a result of increase or decreased apoA-I gene expression. Potential liver damage following adenovirus infection was assessed by measuring serum transaminases using the Reflotron Plus system (Roche). These analyses showed normal serum transaminase levels when mice were infected with 2×10^9 pfu recombinant adenoviruses. Analysis of plasma lipids and apoA-I levels 4 days post-infection showed that compared to WT apoA-I, mice expressing the two mutants had greatly reduced plasma cholesterol levels and reduced plasma CE/TC ratio. Plasma triglycerides and phospholipid levels of mice expressing the two mutants were also reduced compared to mice expressing the WT apoA-I (Table 2). Treatment of apoA-I$^{-/-}$ mice with a control adenovirus expressing the green fluorescent protein (GFP) did not change their plasma lipid levels compared to those of untreated apoA-I$^{-/-}$ mice. FPLC analysis of plasma showed that the HDL cholesterol peak of the mice expressing the two mutants was very small compared to WT apoA-I (Figure 2), while the apoA-I mRNA levels of the two mutants were comparable or even higher for those of WT apoA-I, indicating defective synthesis of HDL (Table 2).

Analysis of the distribution of apoA-I following density gradient ultracentrifugation of plasma showed that in mice infected with adenoviruses expressing the WT apoA-I, apoA-I protein was predominantly distributed in the HDL2 and HDL3 regions (Figure 3A). Consistent with the FPLC data shown in Figure 2, in mice infected with 1×10^9 pfu of the adenoviruses expressing the mutant apoA-I(Leu141Arg)$_{Pisa}$, traces of apoA-I protein were detected in the HDL3 region and the $d > 1.21$ g/mL fraction (Figure 3B). Similar distribution of apoA-I was obtained when mice were infected with 2×10^9 pfu of adenoviruses expressing the apoA-I(Leu141Arg)$_{Pisa}$ mutant (data not shown). In mice infected with the adenoviruses expressing the apoA-I(Leu159Arg)$_{FIN}$ mutant, small amounts of apoA-I were distributed in HDL2 and HDL3 as well as the LDL regions and the $d > 1.21$ g/mL fraction (Figure 3C). To observe detectable apoA-I and lipid levels, it was necessary to use a higher dose (2×10^9 pfu) of the adenovirus expressing this mutant. EM analysis of the HDL fractions 6−8 obtained by density gradient ultracentrifugation (Figure 3A−C) showed that WT apoA-I promoted the formation of spherical particles (Figure 3D), whereas apoA-I(Leu141Arg)$_{Pisa}$ and apoA-I(Leu159Arg)$_{FIN}$ mutants contained very small number of particles (Figure 3E and F). The number of particles generated by the two mutants was similar to that obtained in apoA-I$^{-/-}$ mice or in mice infected with the control adenovirus expressing GFP (Figure 3G). Two-dimensional gel electrophoresis of plasma showed that the WT apoA-I formed α-HDL particles and small amounts of preβ_1-HDL particles. The αHDL to preβ ratio in plasma of apoA-I$^{-/-}$ mice expressing WT apoA-I or the mutants apoA-I(Leu141Arg)$_{Pisa}$ and apoA-I(Leu159Arg)$_{Fin}$ was estimated by scanning densitometry. The ratio was approximately 13 in the case of WT apoA-I (Figure 3H). In the case of the two mutants, the α4-HDL/preβ ratio of apoA-I (Leu141Arg)$_{Pisa}$ and (Leu159Arg)$_{Fin}$ was approximately 3.7 and 2.1, respectively (Figure 3I and J). In both cases of the mutant apoA-I forms, α1, α2, and α3 HDL subpopulations were not formed. A similar profile of HDL subfractions was obtained when mice were infected with 2×10^9 pfu of adenoviruses expressing the apoA-I(Leu141Arg)$_{Pisa}$ mutant (data not shown).

In Vivo Effect of the LCAT on Plasma Lipids, FPLC Profiles, the Distribution of HDL in Different Densities, and the Size and Shape of HDL. To assess how apoA-I mutations affect the biogenesis of HDL, apoA-I$^{-/-}$ mice were co-infected with a mixture of adenoviruses expressing apoA-I(Leu141Arg)$_{Pisa}$ or apoA-I(Leu159Arg)$_{FIN}$ mutants along with human LCAT. The relative levels of expression of the two mutants, as determined by apoA-I mRNA following co-infection, were comparable to or lower than the mRNA levels

Table 2: Analysis of Plasma Lipids and ApoA-I Levels and Hepatic mRNA Levels of ApoA-I$^{-/-}$ Mice, 4 Days Post-Infection with Recombinant Adenoviruses Expressing the WT ApoA-I or ApoA-I Mutants or the Control Protein GFP[a]

protein expressed	cholesterol (TC) (mg/dL)	free cholesterol (mg/dl)	cholesterol esters (CE) (mg/dL)	CE/TC	triglycerides (TG)	phospholipids (P)	relative apoA-I mRNA (%)	apoA-I protein (mg/dL)
apoA-I WT	148 ± 11	32 ± 4	116 ± 7	0.78 ± 0.01	63 ± 1	343 ± 31	100 ± 32	186 ± 34
GFP	38 ± 0.1	18 ± 0.5	20 ± 0.3	0.53 ± 0.01	50 ± 5	26 ± 8		
apoA-I (Leu141Arg)$_{Pisa}$	23 ± 0.4	11 ± 0.4	10 ± 0.8	0.44 ± 0.03	11 ± 2.8	41 ± 1	88 ± 9	17 ± 4
apoA-I (Leu141Arg)$_{Pisa}$ + LCAT	184 ± 53	59 ± 16	125 ± 37	0.68 ± 0.01	41 ± 0.3	50 ± 22	91 ± 2	224 ± 7
apoA-I (Leu159Arg)$_{FIN}$	16 ± 5	14 ± 4	2 ± 1	0.13 ± 0.04	25 ± 4	19 ± 6	216 ± 32	25 ± 9
apoA-I (Leu159Arg)$_{FIN}$ + LCAT	224 ± 22	61 ± 8	163 ± 15	0.73 ± 0.01	53 ± 15	94 ± 30	63 ± 9	190 ± 20
untreated mice								
apoA-I$^{-/-}$	40 ± 2	19 ± 4	21 ± 3	0.53 ± 0.05	27 ± 3	7 ± 2		
C57BL/6	96 ± 16	22 ± 2	74 ± 18	0.76 ± 0.06	19 ± 0.7	170 ± 20		

[a] The values are means ± S.D. (n = 4−6).

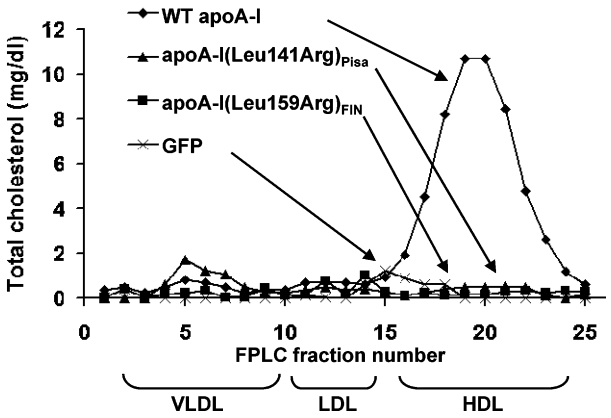

FIGURE 2: FPLC profiles of total cholesterol of apoA-I$^{-/-}$ mice infected with adenoviruses expressing the WT apoA-I (1×10^9 pfu), apoA-I(Leu141Arg)$_{Pisa}$ (1×10^9 pfu), apoA-I(Leu159Arg)$_{FIN}$ (2×10^9 pfu), or the control protein GFP (1×10^9 pfu). Plasma samples were obtained 4 days post-infection.

of mice infected with WT or mutant apoA-I forms alone (Table 2). The co-infection of LCAT, with either of the two mutants, had a dramatic effect on plasma lipids and lipoprotein levels. The LCAT activity of the plasma of mice, 4 days after infection with adenoviruses expressing either the mutant apoA-I(Leu141Arg)$_{Pisa}$ alone or in combination with the human LCAT, was determined using as a substrate rHDL particles containing WT apoA-I. The LCAT catalytic efficiency of the plasma expressed as the ratio of $V\text{max}_{app}$/$K\text{m}_{app}$ was 2.1 nmol(CE)/h/μM apoA-I for mice expressing the mutant apoA-I form alone and 89 nmol(CE)/h/μM apoA-I for mice expressing the mutant apoA-I form in combination with human LCAT.

The mass of LCAT in plasma was estimated by Western blotting using mouse-LCAT antibodies that cross-react efficiently with human LCAT. It was found that in apoA-I$^{-/-}$ mice expressing the control protein GPF, the plasma LCAT was undetectable, but the expression of WT apoA-I greatly increases the mouse LCAT in plasma. In apoA-I$^{-/-}$ mice expressing the mutant apoA-I(Leu141Arg)$_{Pisa}$, the mouse LCAT was also decreased dramatically. The levels of LCAT in plasma were restored to normal levels (those observed in the presence of WT apoA-I) by infection of mice with adenoviruses expressing the mutant form of apoA-I in combination with human LCAT (Figure 4C). In mice co-infected with adenoviruses expressing LCAT and the apoA-I(Leu141Arg)$_{Pisa}$ mutant, there was a 13-, 8-, and 12.5-fold increase in the plasma apoA-I, the total, and the esterified cholesterol, respectively. LCAT treatment also normalized the CE/TC ratio of total plasma and the HDL fraction (Table 2 and Figure 4A, respectively). All of the increase in cholesterol could be attributed to the increase in plasma HDL (Figure 4A). The LCAT co-infection also increased the plasma free cholesterol and triglycerides levels approximately 4-fold (Table 2). In mice co-infected with adenoviruses expressing LCAT and the apoA-I(Leu159Arg)$_{FIN}$ mutant, there was a 7.6-, 14-, and 81-fold increase at the plasma apoA-I, the total, and the esterified cholesterol levels, respectively. The CE/TC ratio of total plasma and the HDL fraction were normalized (Table 2 and Figure 4B, respectively). SDS−PAGE analysis of the fractions obtained by density gradient ultracentrifugation showed that the plasma apoA-I for the two mutants was distributed mostly in the HDL2 and HDL3 region, with small amounts in the lower density fractions. The observed distribution of the mutant apoA-I forms following the LCAT treatment was similar but not identical to the distribution of the WT apoA-I without LCAT treatment (compare Figure 3A with Figure 4D and E). The distribution of apoA-I assessed by ultracentrifugation and SDS−PAGE was also reflected in the distribution of HDL cholesterol of the two mutants relative to WT apoA-I, as determined by FPLC analysis (Figure 4A and B).

Useful information was obtained by comparing the relative distribution of apoA-I, apoE, and apoA-IV in the plasma of mice infected with adenoviruses expressing WT and mutant apoA-I forms with or without concomitant infection with adenoviruses expressing LCAT. In mice expressing the apoA-I(Leu141Arg)$_{Pisa}$ and apoA-I(Leu159Arg)$_{FIN}$, the LCAT treatment increased the concentration of apoE in the HDL2 and LDL regions, and it also increased the concentration of apoA-IV in the HDL3 region (compare Figure 3B and C with Figure 4D and E). The LCAT treatment also promoted the formation of spherical HDL particles similar to those formed by WT apoA-I (compare Figure 3D with Figure 4F

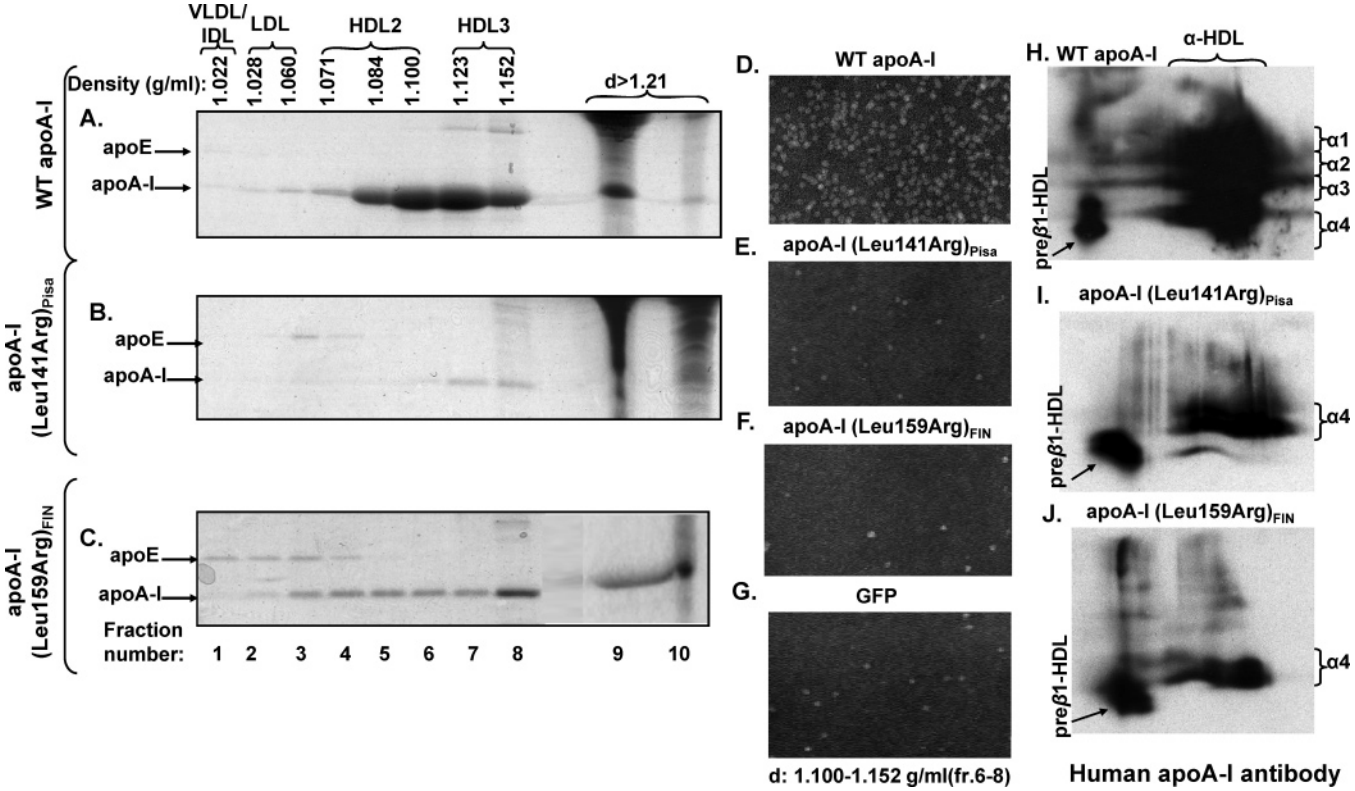

FIGURE 3: (A−J) Analyses of plasma of apoA-I$^{-/-}$ mice infected with adenoviruses expressing the WT apoA-I (A, D, and H), the apoA-I(Leu141Arg)$_{Pisa}$ (B, E, and I), the apoA-I(Leu159Arg)$_{FIN}$ (C, F, and J), or the control adenovirus expressing GFP (G) by density gradient ultracentrifugation, SDS−PAGE, EM, and 2D gel electrophoresis. Panels A−C: SDS−PAGE analysis of density gradient ultracentrifugation fractions. Panels D−G: EM pictures of HDL fractions 6−8 obtained from apoA-I$^{-/-}$ mice expressing the WT apoA-I, the mutant forms, or the control adenovirus expressing GFP following density gradient ultracentrifugation of plasma as indicated. The photomicrographs were taken at 75,000× magnification and enlarged 3 times. Panels H−J: Analysis of plasma obtained from mice expressing the WT apoA-I mutant forms as indicated following 2D gel electrophoresis and Western blotting.

and H). It also normalized the preβ1- to α-HDL ratio of plasma HDL (compare Figure 3I and J with Figure 4G and I). In mice expressing the apoA-I(Leu141Arg)$_{Pisa}$, we observed the formation of preβ1 along with α4, α3, α2, and to a lesser extend α1 particles (Figure 4G). In mice expressing the apoA-I(Leu159Arg)$_{FIN}$, we observed preβ1 along with α3, α2, and α1 particles (Figure 4I).

Figure 5 is a schematic representation showing the pathway of the biogenesis of HDL and how the two mutations affect the esterification of the cholesterol of the preβ-HDL particles, a process that is important for their conversion to discoidal and spherical HDL particles. The figure also shows that if esterification of cholesterol is prevented, then preβ-HDL particles are removed from plasma, thus resulting in low HDL and apoA-I levels.

DISCUSSION

In previous studies, we considered HDL biogenesis as a continuous pathway, where apoA-I and various participating proteins interact successively to form initially preβ-HDL and subsequently discoidal and spherical HDL particles that are biologically active (*5*). The strategy we employed in these studies was adenovirus-mediated gene transfer of apoA-I mutants to apoA-I$^{-/-}$ mice, and it was designed to identify steps in this pathway where intermediates cannot be converted to products and therefore accumulate in plasma (*15*−*19*, *34*) or may be degraded. Discrete phenotypes were thus observed, characterized by defective HDL synthesis due to defective ABCA1/apoA-I interactions, an abnormal preβ-/α-HDL ratio, accumulation of discoidal particles (*15*−*18*, *34*), and various forms of dyslipidemias (*15*−*19*, *34*).

In the present study, we used a similar approach to assess the impact of two naturally occurring apoA-I mutants (apoA-I(Leu141Arg)$_{Pisa}$ and apoA-I(Leu159Arg)$_{FIN}$) on the biogenesis of HDL. The phenotypes produced in this study by adenovirus-mediated gene transfer of the two apoA-I mutants in apoA-I$^{-/-}$ mice were expected to mimic phenotypes previously observed in human patients hemizygotes or heterozygotes for these mutations (*13*, *22*−*26*). The formation of HDL was assessed by FPLC fractionation, 2D gel electrophoresis of plasma, EM analysis, and the CE/TC ratio of the HDL fraction. Other parameters that indicated potential abnormalities in HDL synthesis included the skewed distribution of apoA-I toward the HDL3 region.

Our studies showed that gene transfer of apoA-I(Leu141Arg)$_{Pisa}$ and apoA-I(Leu159Arg)$_{FIN}$ mutants in apoA-I deficient mice resulted in very low total apoA-I and HDL cholesterol, formation of preβ-HDL and α4-HDL particles of fast electrophoretic mobility, a very small number of spherical HDL particles, as determined by EM, and a decreased CE/TC ratio of plasma and the HDL fraction. Previous studies with human subjects showed that hemizygotes (compound heterozygotes for an apoA-I null allele and an apoA-I(Leu141Arg)$_{Pisa}$ allele) had greatly decreased plasma apoA-I levels and near absence of HDL cholesterol, whereas heterozygotes for apoA-I(Leu141Arg)$_{Pisa}$ had approximately half-normal values for HDL cholesterol and plasma apoA-I (*22*, *25*). Plasma from hemizygotes contained

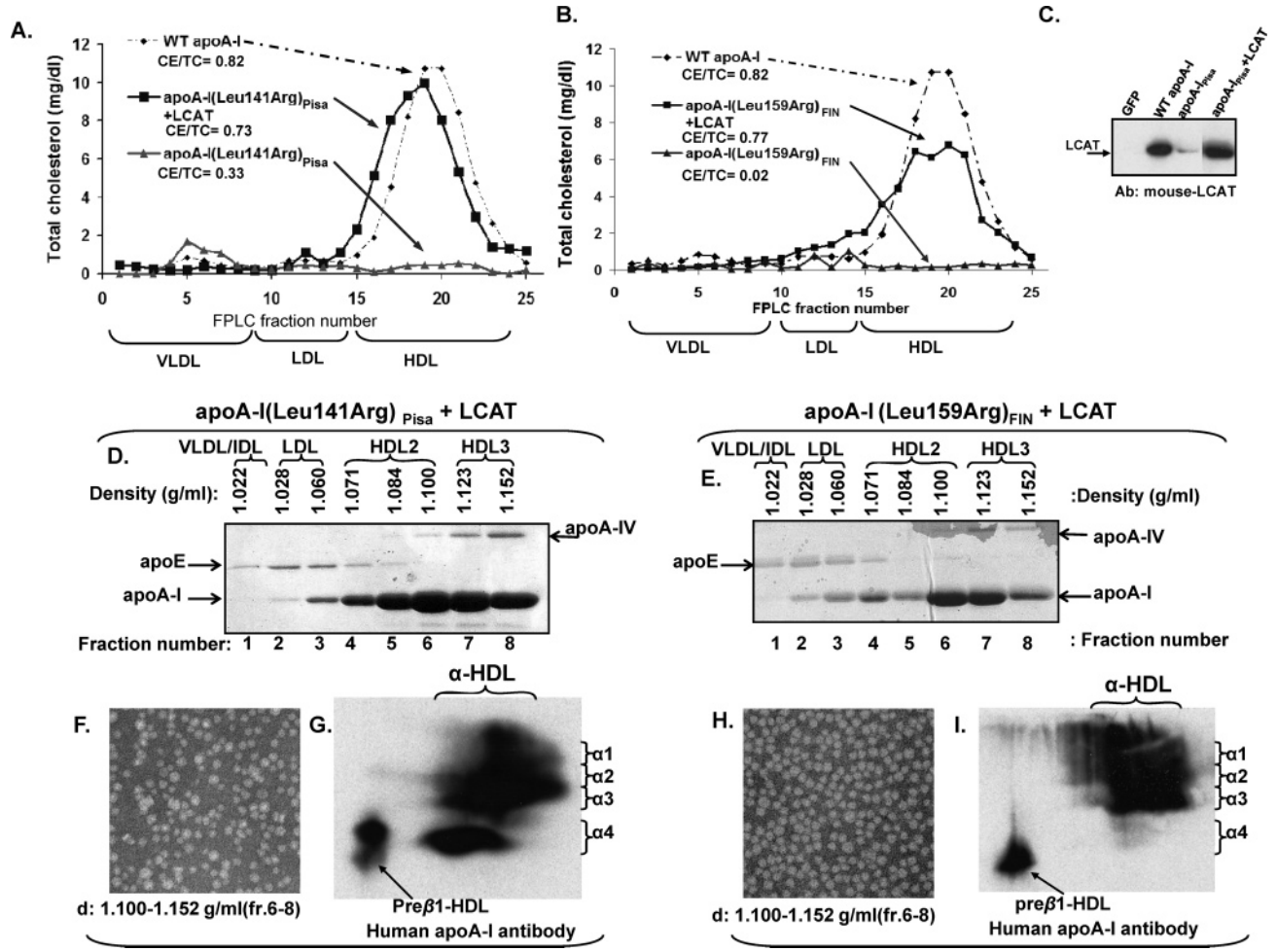

FIGURE 4: (A−I) Analyses of plasma of apoA-I$^{-/-}$ mice infected with a combination of adenoviruses expressing human LCAT (5×10^8 pfu) and apoA-I(Leu141Arg)$_{Pisa}$ (1×10^9 pfu) or the apoA-I(Leu159Arg)$_{FIN}$ (2×10^9 pfu). Panels A and B: FPLC profiles as indicated. The CE/TC ratio of the HDL fractions 15−22 of the FPLC is indicated. Panel C: Western blot analysis of plasma from apoA-I$^{-/-}$ mice infected with adenoviruses expressing either the control protein, GFP, or the WT apoA-I or the apoA-I(Leu141Arg)$_{Pisa}$ alone or in combination with human LCAT, as indicated at the top of the figure. An aliquot of 0.5 mL of plasma was analyzed. The blot was probed with rabbit anti-mouse-LCAT antibody, which cross-reacts with both human and mouse LCAT. Panels D and E: SDS−PAGE profiles of fractions obtained by density gradient ultracentrifugation analysis of plasma of apoA-I$^{-/-}$ mice expressing the mutant forms of apoA-I in combination with the human LCAT, as indicated. Panels F and H: EM pictures of HDL fractions 6−8 obtained from apoA-I$^{-/-}$ mice expressing the indicated mutant forms in combination with human LCAT, following density gradient ultracentrifugation of plasma as indicated. The photomicrographs were taken at 75,000× magnification and enlarged 3 times. Panels G and I: Analysis of plasma obtained from mice expressing the indicated mutant forms in combination with human LCAT following 2D gel electrophoresis and Western blotting.

preβ1-HDL and a low concentration of small particles with α-electrophoretic mobility (*23*). Three male hemizygote patients and one heterozygote patient developed coronary stenosis (*22*).

The findings of low plasma and HDL cholesterol levels in mice expressing apoA-I(Leu141Arg)$_{Pisa}$ and the preponderance of preβ- and fast migrating α4-HDL particles are in agreement with previous studies (*22*, *23*, *25*) and indicate that adenovirus-mediated gene transfer represents an efficient way to reproduce abnormal phenotypes that result from mutations in apoA-I. The apoA-I(Leu159Arg)$_{FIN}$ phenotype observed in our studies has characteristics identical to that of apoA-I(Leu141Arg)$_{Pisa}$.

Previous studies showed that heterozygotes for apoA-I(Leu159Arg)$_{FIN}$ mutation or mice infected with adenovirus expressing apoA-I(Leu159Arg)$_{FIN}$ had greatly reduced plasma levels of HDL cholesterol and apoA-I (*24*), which was mainly distributed in the HDL3 (*13*). They also had small size (8−9 nm) HDL particles and decreased plasma and HDL cholesteryl ester levels (*13*, *33*). Native−PAGE of plasma from mice infected with adenoviruses expressing the apoA-I(Leu159 Arg)$_{FIN}$ mutant indicated that HDL consisted of particles with preβ-electrophoretic mobility as well as particles with electrophoretic mobility between α and preβ (*33*). These particles were not analyzed by 2D electrophoresis, but their migration is compatible with the α4-HDL particles observed in our study. Human HDL containing apoA-I(Leu159Arg)$_{FIN}$ had an increased fractional catabolic rate compared to that of normal HDL, indicating increased catabolism of the mutant apoA-I protein (*13*, *24*). Only one affected patient with this mutation had clinically manifested atherosclerosis (*13*).

LCAT Treatment Can Correct the HDL Abnormalities Brought about by the Mutations ApoA-I(Leu141Arg)$_{Pisa}$ and ApoA-I(Leu159Arg)$_{FIN}$ and Suggest a Mechanism Responsible for the HDL Deficiency Observed in Human Patients Carrying These Mutations. Insights into the molecular etiology of the low HDL levels observed in patients with apoA-I(Leu141Arg)$_{Pisa}$ and apoA-I(Leu159Arg)$_{FIN}$ were provided by treatment of apoA-I$^{-/-}$ mice with a combination

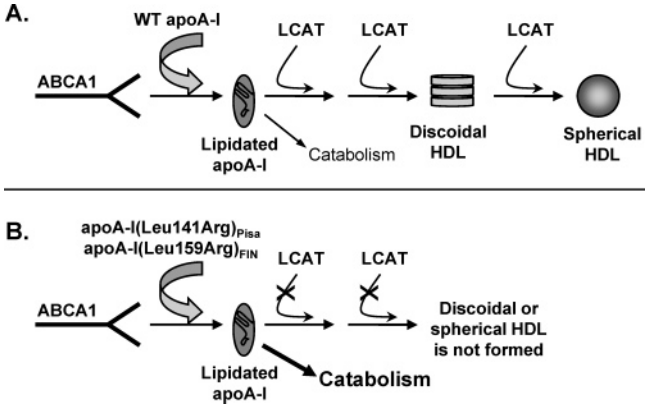

FIGURE 5: Schematic representation showing the pathway of biogenesis of HDL and how the two mutations affect the esterification of cholesterol of the preβ-HDL particles and prevent their conversion to discoidal and spherical HDL, thus promoting their catabolism.

of adenoviruses expressing either of the two mutants and human LCAT. This treatment corrected the plasma apoA-I and HDL levels, normalized the CE/TC ratio, restored normal preβ- and α-HDL subpopulations, and led to the formation of spherical HDL particles.

The restoration of normal levels of apoA-I and HDL following treatment with LCAT supports the notion that apoA-I mutants are secreted efficiently by the liver but that the ability of the endogenous LCAT to esterify the cholesterol of the newly formed preβ-particles is rate-limiting. The *in vivo* data are also supported by cell culture studies and *in vitro* functional assays of apoA-I. Thus, the present study as well as a previous study (*33*) indicated that both mutant proteins could be secreted efficiently from cell cultures and that they had normal ability to promote ABCA1-dependent cholesterol efflux from J774 macrophages stimulated with a cAMP analogue but had reduced ability to activate LCAT *in vitro* (*13*, *33*).

Previous studies showed that preβ-HDL is an efficient substrate of LCAT (*35*). Because of LCAT insufficiency, it appears that the nascent lipidated apoA-I that is produced by functional interactions of apoA-I with ABCA1 is removed fast from the plasma compartment. This interpretation is supported by the increased catabolic rate of HDL containing apoA-I(Leu159Arg)$_{FIN}$ (*13*) and the accumulation of proapoA-I in the plasma of hemizygotes for apoA-I(L141R)$_{Pisa}$ (*22*). Accumulation of proapoA-I has been previously observed in patients with Tangier disease (*36*) that is characterized by increase catabolic rate of HDL (*2*). Increased degradation of preβ-HDL has been observed in mice with liver specific inactivation of ABCA1 (*37*, *38*). It has been shown previously that cubulin, a 600 KDa membrane protein, binds both apoA-I and HDL and promotes their catabolism by the kidney (*39*, *40*). Analysis of the relative abundance of endogenous LCAT in apoA-I$^{-/-}$ mice expressing the mutant apoA-I(Leu141Arg)$_{Pisa}$ showed that it was also decreased dramatically compared to mice expressing WT apoA-I but was restored to normal levels (those observed in the presence of WT apoA-I) by infection of mice with adenoviruses expressing the mutant form of apoA-I in combination with human LCAT. The depletion of the endogenous LCAT in mice expressing the mutant forms of apoA-I could be the result of rapid degradation of endogenous mouse LCAT bound to minimally lipidated apoA-I mutants.

In the presence of excess LCAT, the esterification of the cholesterol of the newly formed preβ-particles appears to prevent their fast catabolism and allows them to proceed in the formation of discoidal and spherical HDL. We have previously shown that a substitution of Arg160Ala/His162Val of apoA-I prevented the esterification of the cholesterol of the discoidal HDL and resulted in the accumulation discoidal HDL in plasma (*17*). Thus, in this case, the metabolic block was the conversion of the discoidal to spherical HDL. The present study establishes for the first time that the apoA-I(Leu141Arg)$_{Pisa}$ and apoA-I(Leu159Arg)$_{FIN}$ mutations inhibit an earlier step in the biogenesis of HDL that precedes the formation of discoidal HDL particles (Figure 5).

Taken together with previous studies, our data suggest that following the initial lipidation of apoA-I, LCAT fails to esterify the cholesterol of preβ particles (Figures 1B and 3A−J) (*13*, *22*−*25*, *33*). This leads to the fast removal of preβ-HDL from plasma and a decrease in the plasma HDL levels (*13*, *23*, *24*, *39*, *40*). The correction of the aberrant HDL phenotypes by treatment with LCAT suggests a potential therapeutic intervention for HDL abnormalities that result from specific mutations in apoA-I.

ACKNOWLEDGMENT

We thank Dr. Silvia Santamarina-Fojo for providing the adenovirus expressing the human LCAT. We thank Dr. John Parks for providing the mouse LCAT and human LCAT antibodies. We thank Anne Plunkett for preparing the manuscript and Gayle Forbes for technical assistance.

REFERENCES

1. Karathanasis, S. K., Zannis, V. I., and Breslow, J. L. (1983) Isolation and characterization of the human apolipoprotein A-I gene, *Proc. Natl. Acad. Sci. U.S.A 80*, 6147−6151.
2. Assmann, G., von Eckardstein, A., and Brewer, H. B. (2001) in *The Metabolic and Molecular Basis of Inherited Disease* (Scriver, C. R., Beaudet, A. L., Sly, W. S., and Valle, D., Eds.) pp 2937−2960, McGraw-Hill, New York.
3. Williamson, R., Lee, D., Hagaman, J., and Maeda, N. (1992) Marked reduction of high density lipoprotein cholesterol in mice genetically modified to lack apolipoprotein A-I, *Proc. Natl. Acad. Sci. U.S.A 89*, 7134−7138.
4. Matsunaga, T., Hiasa, Y., Yanagi, H., Maeda, T., Hattori, N., Yamakawa, K., Yamanouchi, Y., Tanaka, I., Obara, T., and Hamaguchi, H. (1991) Apolipoprotein A-I deficiency due to a codon 84 nonsense mutation of the apolipoprotein A-I gene, *Proc. Natl. Acad. Sci. U.S.A 88*, 2793−2797.
5. Zannis, V. I., Chroni, A., and Krieger, M. (2006) Role of apoA-I, ABCA1, LCAT, and SR-BI in the biogenesis of HDL, *J. Mol. Med. 84*, 276−294.
6. Krieger, M. (2001) Scavenger receptor class B type I is a multiligand HDL receptor that influences diverse physiologic systems, *J. Clin. Invest 108*, 793−797.
7. Wang, N., Lan, D., Chen, W., Matsuura, F., and Tall, A. R. (2004) ATP-binding cassette transporters G1 and G4 mediate cellular cholesterol efflux to high-density lipoproteins, *Proc. Natl. Acad. Sci. U.S.A 101*, 9774−9779.
8. Jiang, X. C., Bruce, C., Mar, J., Lin, M., Ji, Y., Francone, O. L., and Tall, A. R. (1999) Targeted mutation of plasma phospholipid transfer protein gene markedly reduces high-density lipoprotein levels, *J. Clin. Invest. 103*, 907−914.
9. Chajek, T., and Fielding, C. J. (1978) Isolation and characterization of a human serum cholesteryl ester transfer protein, *Proc. Natl. Acad. Sci. U.S.A 75*, 3445−3449.
10. Miller, M., Aiello, D., Pritchard, H., Friel, G., and Zeller, K. (1998) Apolipoprotein A-I(Zavalla) (Leu159→Pro): HDL cholesterol deficiency in a kindred associated with premature coronary artery disease, *Arterioscler., Thromb., Vasc. Biol. 18*, 1242−1247.

11. Hovingh, G. K., Brownlie, A., Bisoendial, R. J., Dube, M. P., Levels, J. H., Petersen, W., Dullaart, R. P., Stroes, E. S., Zwinderman, A. H., de Groot, E., Hayden, M. R., Kuivenhoven, J. A., and Kastelein, J. J. (2004) A novel apoA-I mutation (L178P) leads to endothelial dysfunction, increased arterial wall thickness, and premature coronary artery disease. *J. Am. Coll. Cardiol. 44*, 1429−1435.
12. Sorci-Thomas, M. G., and Thomas, M. J. (2002) The effects of altered apolipoprotein A-I structure on plasma HDL concentration, *Trends Cardiovasc. Med. 12*, 121−128.
13. Miettinen, H. E., Jauhiainen, M., Gylling, H., Ehnholm, S., Palomaki, A., Miettinen, T. A., and Kontula, K. (1997) Apolipoprotein A-IFIN (Leu159→Arg) mutation affects lecithin cholesterol acyltransferase activation and subclass distribution of HDL but not cholesterol efflux from fibroblasts, *Arterioscler., Thromb., Vasc. Biol. 17*, 3021−3032.
14. Huang, W., Sasaki, J., Matsunaga, A., Nanimatsu, H., Moriyama, K., Han, H., Kugi, M., Koga, T., Yamaguchi, K., and Arakawa, K. (1998) A novel homozygous missense mutation in the apo A-I gene with apo A-I deficiency, *Arterioscler., Thromb., Vasc. Biol. 18*, 389−396.
15. Chroni, A., Liu, T., Gorshkova, I., Kan, H. Y., Uehara, Y., von Eckardstein, A., and Zannis, V. I. (2003) The central helices of apoA-I can promote ATP-binding cassette transporter A1 (ABCA1)-mediated lipid efflux. Amino acid residues 220−231 of the wild-type apoA-I are required for lipid efflux in vitro and high density lipoprotein formation in vivo, *J. Biol. Chem. 278*, 6719−6730.
16. Chroni, A., Koukos, G., Duka, A., and Zannis, V. I. (2007) The carboxy-terminal region of apoA-I is required for the ABCA1-dependent formation of α-HDL but not preβ-HDL particles in vivo, *Biochemistry 46*, 5697−5708.
17. Chroni, A., Duka, A., Kan, H. Y., Liu, T., and Zannis, V. I. (2005) Point mutations in apolipoprotein A-I mimic the phenotype observed in patients with classical lecithin:cholesterol acyltransferase deficiency, *Biochemistry 44*, 14353−14366.
18. Chroni, A., Kan, H. Y., Shkodrani, A., Liu, T., and Zannis, V. I. (2005) Deletions of helices 2 and 3 of human apoA-I are associated with severe dyslipidemia following adenovirus-mediated gene transfer in apoA-I-deficient mice, *Biochemistry 44*, 4108−4117.
19. Chroni, A., Kan, H. Y., Kypreos, K. E., Gorshkova, I. N., Shkodrani, A., and Zannis, V. I. (2004) Substitutions of glutamate 110 and 111 in the middle helix 4 of human apolipoprotein A-I (apoA-I) by alanine affect the structure and in vitro functions of apoA-I and induce severe hypertriglyceridemia in apoA-I-deficient mice, *Biochemistry 43*, 10442−10457.
20. Yamakawa-Kobayashi, K., Yanagi, H., Fukayama, H., Hirano, C., Shimakura, Y., Yamamoto, N., Arinami, T., Tsuchiya, S., and Hamaguchi, H. (1999) Frequent occurrence of hypoalphalipoproteinemia due to mutant apolipoprotein A-I gene in the population: a population-based survey, *Hum. Mol. Genet. 8*, 331−336.
21. Ajees, A. A., Anantharamaiah, G. M., Mishra, V. K., Hussain, M. M., and Murthy, H. M. (2006) Crystal structure of human apolipoprotein A-I: insights into its protective effect against cardiovascular diseases, *Proc. Natl. Acad. Sci. U.S.A 103*, 2126−2131.
22. Miccoli, R., Bertolotto, A., Navalesi, R., Odoguardi, L., Boni, A., Wessling, J., Funke, H., Wiebusch, H., Eckardstein, A., and Assmann, G. (1996) Compound heterozygosity for a structural apolipoprotein A-I variant, apo A-I(L141R)Pisa, and an apolipoprotein A-I null allele in patients with absence of HDL cholesterol, corneal opacifications, and coronary heart disease, *Circulation 94*, 1622−1628.
23. Miccoli, R., Zhu, Y., Daum, U., Wessling, J., Huang, Y., Navalesi, R., Assmann, G., and von Eckardstein, A. (1997) A natural apolipoprotein A-I variant, apoA-I (L141R)Pisa, interferes with the formation of alpha-high density lipoproteins (HDL) but not with the formation of pre beta 1-HDL and influences efflux of cholesterol into plasma, *J. Lipid Res. 38*, 1242.
24. Miettinen, H. E., Gylling, H., Miettinen, T. A., Viikari, J., Paulin, L., and Kontula, K. (1997) Apolipoprotein A-IFin. Dominantly inherited hypoalphalipoproteinemia due to a single base substitution in the apolipoprotein A-I gene, *Arterioscler., Thromb., Vasc. Biol. 17*, 83−90.
25. Pisciotta, L., Miccoli, R., Cantafora, A., Calabresi, L., Tarugi, P., Alessandrini, P., Bittolo, B. G., Franceschini, G., Cortese, C., Calandra, S., and Bertolini, S. (2003) Recurrent mutations of the apolipoprotein A-I gene in three kindreds with severe HDL deficiency, *Atherosclerosis 167*, 335−345.
26. Navalesi, R., Miccoli, R., Odoguardi, L., Funke, H., von Eckardstein, A., Wiebusch, H., and Assmann, G. (1995) Genetically determined absence of HDL-cholesterol and coronary atherosclerosis, *Lancet 346*, 708−709.
27. Gylling, H., Relas, H., Miettinen, H. E., Radhakrishnan, R., and Miettinen, T. A. (1996) Delayed postprandial retinyl palmitate and squalene removal in a patient heterozygous for apolipoprotein A-IFIN mutation (Leu 159→Arg) and low HDL cholesterol level without coronary artery disease, *Atherosclerosis 127*, 239−243.
28. Roghani, A., and Zannis, V. I. (1988) Alterations of the glutamine residues of human apolipoprotein AI propeptide by in vitro mutagenesis. Characterization of the normal and mutant protein forms, *Biochemistry 27*, 7428−7435.
29. Laccotripe, M., Makrides, S. C., Jonas, A., and Zannis, V. I. (1997) The carboxyl-terminal hydrophobic residues of apolipoprotein A-I affect its rate of phospholipid binding and its association with high density lipoprotein, *J. Biol. Chem. 272*, 17511−17522.
30. Amar, M. J. A., Shamburek, R. D., Foger, B., Hoyt, R. F., Wood, D. O., Santamarina-Fojo, S., and Brewer, H. B. (1998) Adenovirus-mediated expression of LCAT in non-human primates leads to an antiatherogenic lipoprotein profile with increased HDL and decreased LDL, *Circulation 98*, 35.
31. Matz, C. E., and Jonas, A. (1982) Micellar complexes of human apolipoprotein A-I with phosphatidylcholines and cholesterol prepared from cholate-lipid dispersions, *J. Biol. Chem. 257*, 4535−4540.
32. Kypreos, K. E., and Zannis, V. I. (2007) Pathway of biogenesis of apolipoprotein E-containing HDL in vivo with the participation of ABCA1 and LCAT, *Biochem, J. 403*, 359−367.
33. McManus, D. C., Scott, B. R., Franklin, V., Sparks, D. L., and Marcel, Y. L. (2001) Proteolytic degradation and impaired secretion of an apolipoprotein A-I mutant associated with dominantly inherited hypoalphalipoproteinemia, *J. Biol. Chem. 276*, 21292−21302.
34. Reardon, C. A., Kan, H. Y., Cabana, V., Blachowicz, L., Lukens, J. R., Wu, Q., Liadaki, K., Getz, G. S., and Zannis, V. I. (2001) In vivo studies of HDL assembly and metabolism using adenovirus-mediated transfer of ApoA-I mutants in ApoA-I-deficient mice, *Biochemistry 40*, 13670−13680.
35. Nakamura, Y., Kotite, L., Gan, Y., Spencer, T. A., Fielding, C. J., and Fielding, P. E. (2004) Molecular mechanism of reverse cholesterol transport: reaction of pre-beta-migrating high-density lipoprotein with plasma lecithin/cholesterol acyltransferase, *Biochemistry 43*, 14811−14820.
36. Zannis, V. I., Lees, A. M., Lees, R. S., and Breslow, J. L. (1982) Abnormal apoprotein A-I isoprotein composition in patients with Tangier disease, *J. Biol. Chem. 257*, 4978−4986.
37. Timmins, J. M., Lee, J. Y., Boudyguina, E., Kluckman, K. D., Brunham, L. R., Mulya, A., Gebre, A. K., Coutinho, J. M., Colvin, P. L., Smith, T. L., Hayden, M. R., Maeda, N., and Parks, J. S. (2005) Targeted inactivation of hepatic Abca1 causes profound hypoalphalipoproteinemia and kidney hypercatabolism of apoA-I, *J. Clin. Invest. 115*, 1333−1342.
38. Singaraja, R. R., Stahmer, B., Brundert, M., Merkel, M., Heeren, J., Bissada, N., Kang, M., Timmins, J. M., Ramakrishnan, R., Parks, J. S., Hayden, M. R., and Rinninger, F. (2006) Hepatic ATP-binding cassette transporter A1 is a key molecule in high-density lipoprotein cholesteryl ester metabolism in mice, *Arterioscler., Thromb., Vasc. Biol. 26*, 1821−1827.
39. Kozyraki, R., Fyfe, J., Kristiansen, M., Gerdes, C., Jacobsen, C., Cui, S., Christensen, E. I., Aminoff, M., de la, C. A., Krahe, R., Verroust, P. J., and Moestrup, S. K. (1999) The intrinsic factor-vitamin B12 receptor, cubilin, is a high-affinity apolipoprotein A-I receptor facilitating endocytosis of high-density lipoprotein, *Nat. Med. 5*, 656−661.
40. Hammad, S. M., Stefansson, S., Twal, W. O., Drake, C. J., Fleming, P., Remaley, A., Brewer, H. B., Jr., and Argraves, W. S. (1999) Cubilin, the endocytic receptor for intrinsic factor-vitamin B(12) complex, mediates high-density lipoprotein holoparticle endocytosis, *Proc. Natl. Acad. Sci. U.S.A. 96*, 10158−10163.

BI7003203